LUNAR SUNRISE ORBITS AND APPLICATIONS TO NASA CLPS MISSIONS

2026 AAS/AIAA Astrodynamics Specialist Conference, Whistler, British Columbia, July 26-30, 2026

By

Anthony L. Genova, NASA CLPS Astrodynamics Subject Matter Expert, Spaceflight Div., NASA Ames Research Ctr., Moffett Field, CA

Dylan Morrison-Fogel, Spaceflight Dynamicist, Axient, NASA Ames Research Ctr., Spaceflight Division, Moffett Field, CA

Ryan P. Russell, Professor, Hayden Head Centennial Professorship, Cockrell School of Eng., The Univ. of Texas at Austin, Austin, TX

Carter J. Van Hammond, Masters Student, Cockrell School of Engineering, The University of Texas at Austin, Austin, TX

Regina Blue, NASA CLPS Deputy Programmatic Manager, NASA Johnson Space Center, NASA, Houston, TX

Executive Summary

*** NASA's Commercial Lunar Payload Services (CLPS) initiative has stimulated the lunar economy with recent and planned landings on the Moon by U.S. companies.**

* **Primary Purpose**: discover, and analyze Lunar Sunrise Orbits (LSOs), sun-synchronous and near repeat ground orbits at the Moon that are phased for a spacecraft to encounter a landing site at sunrise.

* **Lunar sunrise orbits (LSOs)** are defined as orbits with near repeat ground tracks that pass over a specified lunar surface site at successive lunar sunrise times. CLPS landers generally land at (or shortly after) local lunar sunrise to ensure that most of the lunar day can be used for surface operations given the challenges of surviving the cold lunar night.

* For an arbitrary staging orbit, if a lunar descent is delayed for any reason, the spacecraft will approximately return to the landing site after the moon completes 1 synodic revolution. However, the return geometry defined by the spacecraft, landing site, and terminator is not exact due to inertial rotation of the terminator, and due to perturbations from the Earth and the non-spherical gravity of the Moon.

* By utilizing one or more of these LSOs, mission resiliency can be achieved by ensuring existence of backup landing windows at lunar sunrise in case the descent orbit initiation (DOI) and/or associated maneuvers are missed for any reason (e.g., temporary loss of communication, thruster malfunctions, maneuver execution errors, orbit determination problem, off-nominal attitude profile, landing site problems, etc.).

CONTENTS

REPRESENTATIVE
LUNAR SUNRISE ORBIT RESULTS

REPRESENTATIVE
LUNAR SUNRISE ORBIT RESULTS

Lunar Sunrise Orbit Design for Repeatable CLPS Landing Opportunities

* Developed a **medium-fidelity Hamiltonian framework (RTBP+NS)** combining averaged Earth third-body perturbations with high-degree GRAIL lunar gravity to identify lunar repeat ground-track sun-synchronous orbit (LSO) families.

* Introduced **Lunar Sunrise Orbits (LSOs)** as repeat ground-track, sun-synchronous staging orbits that repeatedly revisit a landing region near the local sunrise terminator.

* Demonstrated that appropriately phased LSOs provide a **built-in monthly contingency opportunity** following a missed landing attempt while preserving both landing-site geometry and illumination conditions.\

* Classified four LSO families and identified the **low-altitude** and **classic frozen** families as the most operationally relevant for CLPS and other short-duration lunar surface missions.

* Representative solutions exhibit stable, repeatable behavior with long operational lifetimes while maintaining favorable access to targeted landing regions.

REPRESENTATIVE
LUNAR SUNRISE ORBIT RESULTS

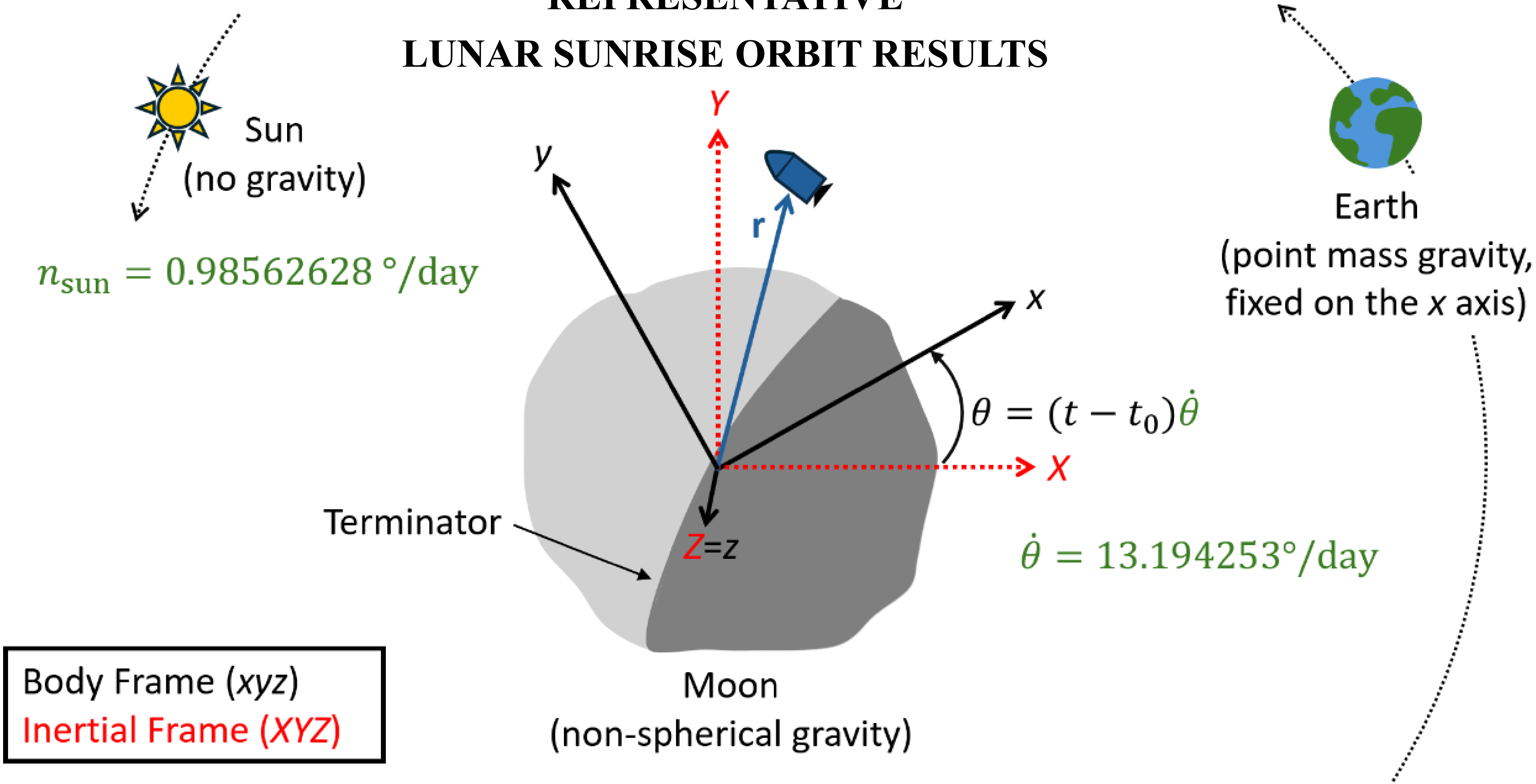

Figure 1. Geometry and notation for the RTBP+NS model

REPRESENTATIVE LUNAR SUNRISE ORBIT RESULTS

Medium-fidelity dynamical model combining averaged Earth perturbations with high-degree lunar gravity to search for repeat ground-track lunar sunrise orbits

N: Integer number of full precessions of the spacecraft orbital plane relative to the Earth-Moon line.
M: Integer number of spacecraft revolutions about the Moon

Orbital elements remain tightly bounded over an entire repeat cycle, demonstrating repeatable long-duration behavior

Short-period oscillations remain well controlled, with only minimal secular drift

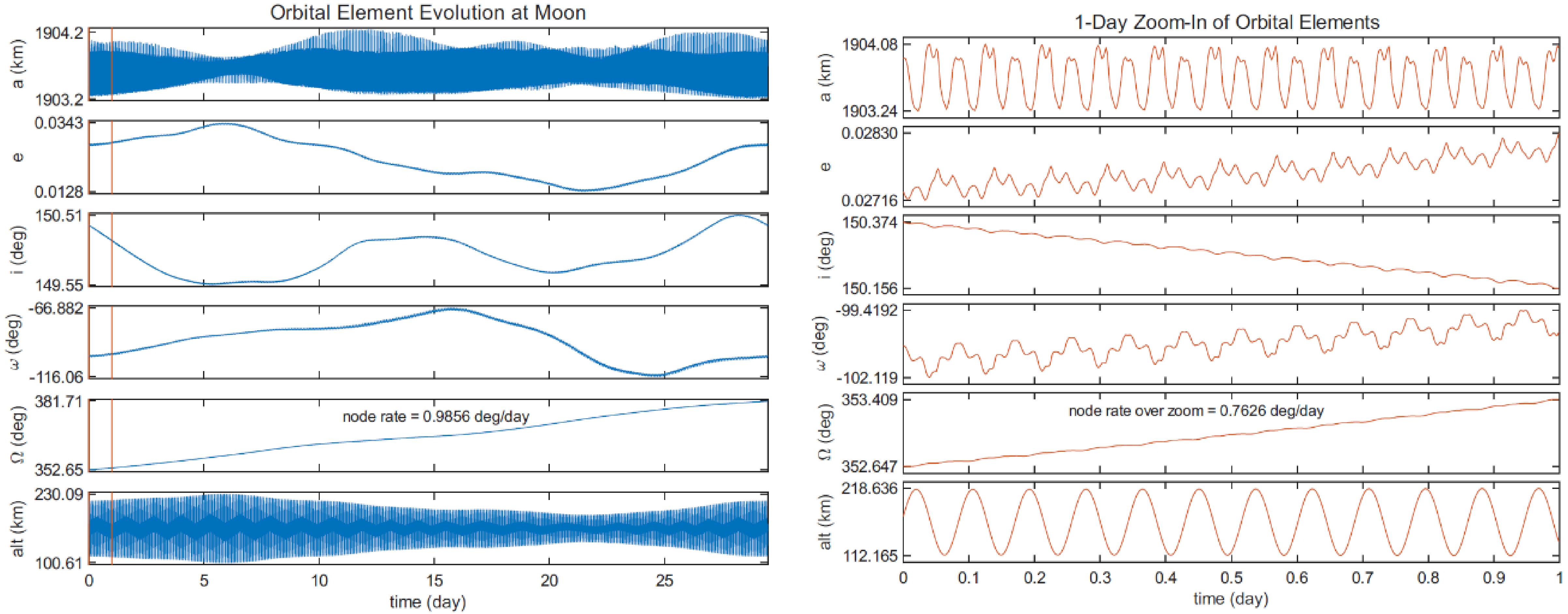

Figure 2: Representative $N = 342$ low-altitude LSO.

b1 = 1.4652120168901004 & b2 = 2.0023837677614287

REPRESENTATIVE
LUNAR SUNRISE ORBIT RESULTS

N: Integer number of full precessions of the spacecraft orbital plane relative to the Earth-Moon line.
M: Integer number of spacecraft revolutions about the Moon

The orbit repeatedly revisits the same mid-latitude landing region approximately once per synodic month

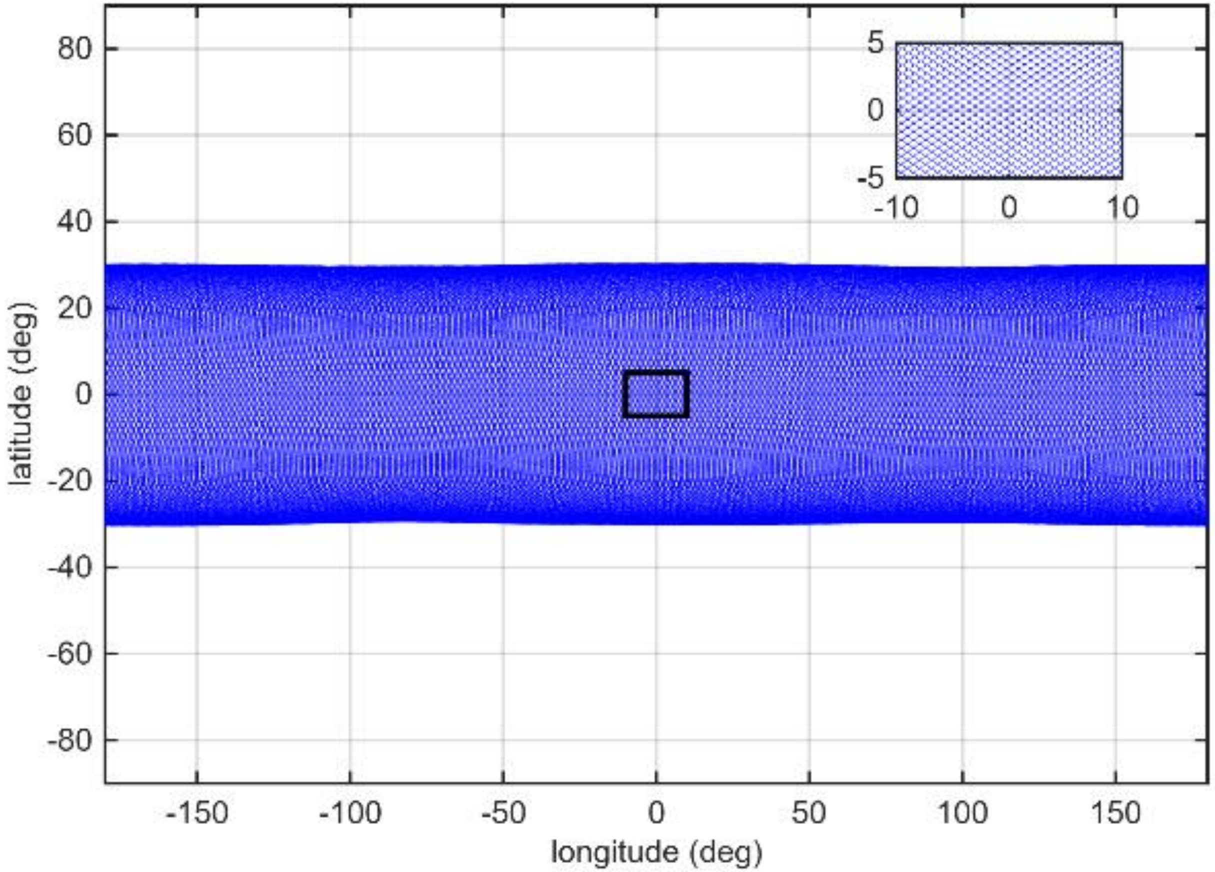

The eccentricity vector follows a bounded periodic trajectory, confirming linear stability of the solution

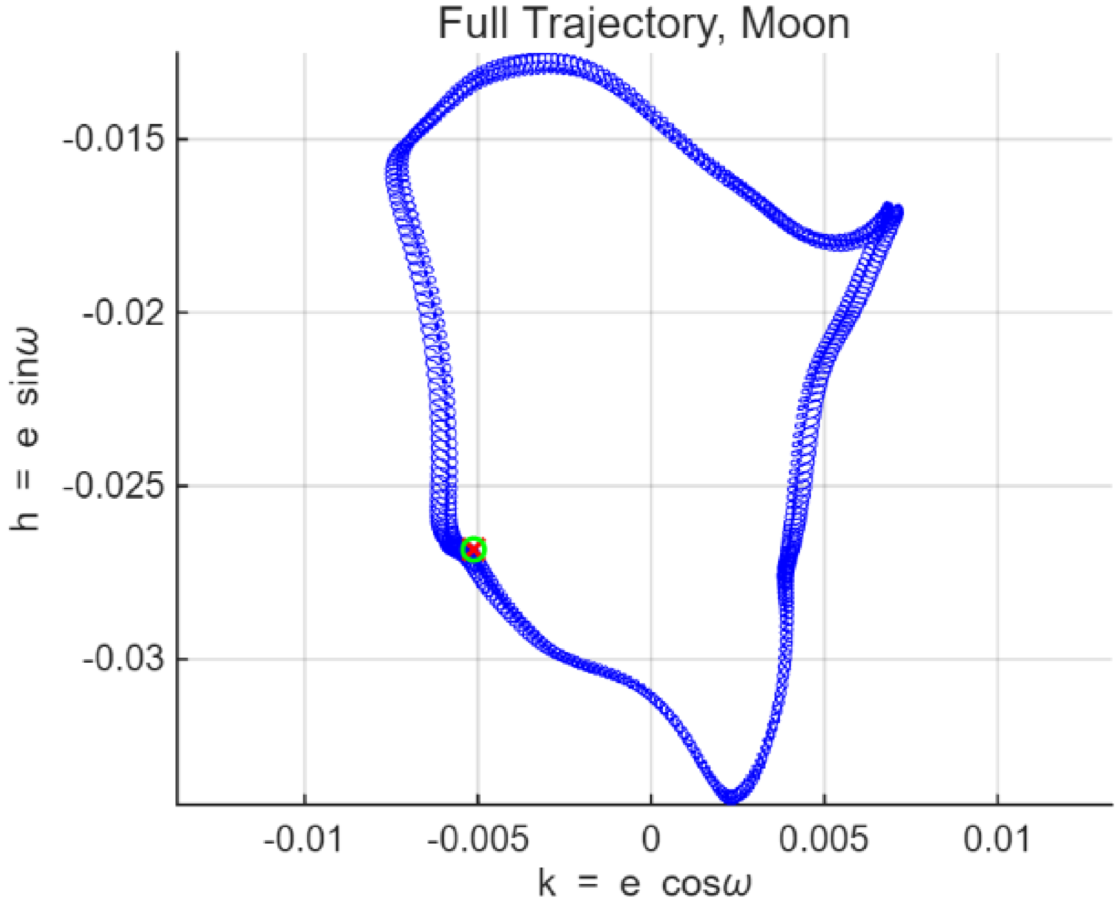

Figure 2: Representative $N = 342$ low-altitude LSO.

b1 = 1.4652120168901004 & b2 = 2.0023837677614287

NUMERICAL HIGH-FIDELITY SEARCH with STK

NUMERICAL HIGH-FIDELITY SEARCH with STK

For the numerical scan to follow, the perilune altitude is set to 100 km given its proximity to the previously studied 95X206 km frozen LLO [11] and since most LLOs and lander missions utilize an altitude of ~100 km.

To determine the initial apolune altitude to use in the numerical scan, using the same assumptions and constraints from [11], an apolune scan from 210 to 500 km was performed.

It was found that the lowest range in $RAAN_{Moon\text{-}Sun}$, for most values of initial lunar orbit inclination, was yielded when apolune altitude = 210 km (Fig. 4), which closely resembles the (N=342, M=1) case discussed in the companion paper.

Table 1. Numerical High-Fidelity Search Assumptions & Constraints

Parameter	Assumptions & Constraints
Spacecraft	Mass = 1,000 kg, Maximum Cross-Sectional Surface Area = 5 m^2
Force Model	100X100 Moon; 30X30 Earth; 4X0 Sun; Point Masses for all other planets; Spherical Radiation Pressure
Numerical Integrator	RKF78 with Max Abs Error = 1E-13 and Maximum Relative Error = 1E-13
Initial Fixed Orbital Elements	Epoch: Jan. 4, 2027, Perilune Altitude = 100 km, Apolune Altitude = 210 km, ω = 270 deg
Propagation Duration in STK	14 days (or STOP on impact)
Design Variables (Varied parameters)	*inclination from 0.5 to 179.5 deg in 0.5 deg increments;* LAN: 0 to 360 deg. in 30-degree increments; 4,308 cases (359*12)
Primary Response Variables	Range of $RAAN_{Moon\text{-}Sun}$, Orbital Elements, & Orbit Lifetime

RAAN (Moon-Sun)

* RAAN was specifically analyzed in the Moon-Sun rotating frame, ($\mathcal{F}_{Moon-Sun}$)

* To define this frame, we adopt the convention of the x-axis aligning with the Moon-Sun vector, the z-axis aligning with the Moon's angular momentum about the Sun, and the y-axis completing the right-handed system

* We define the $RAAN_{Moon-Sun}$ angle as the dihedral angle from the $\mathcal{F}_{Moon-Sun}$ x-axis to the ascending node of a lunar orbit, measured about the $\mathcal{F}_{Moon-Sun}$ z-axis

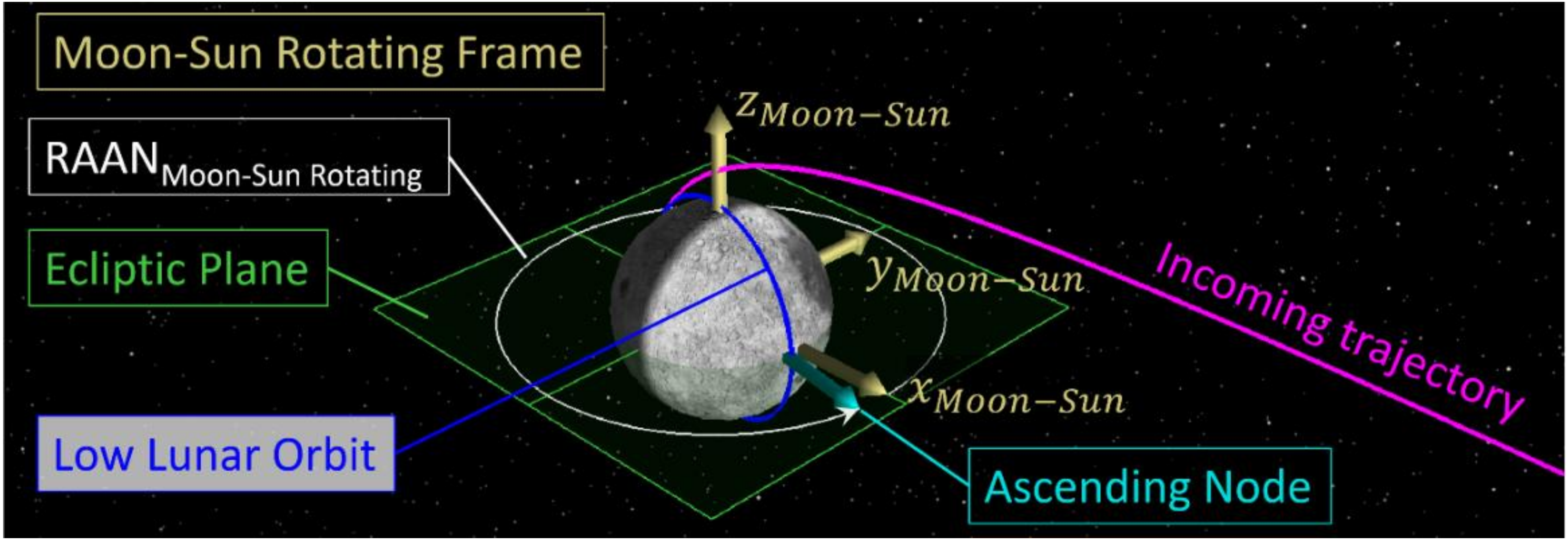

Diagram illustrating the $\boldsymbol{RAAN_{Moon-Sun}}$ angle. From: Genova, A. L., Morrison-Fogel, D., & Levinson-Muth, P., "Transfers from TLI to Lunar Frozen Orbits with Applications to NASA's CLPS & Artemis Programs," AAS/AIAA Space Flight Mech. Mtg., Orlando, FL, Jan. 8-12, 2024.

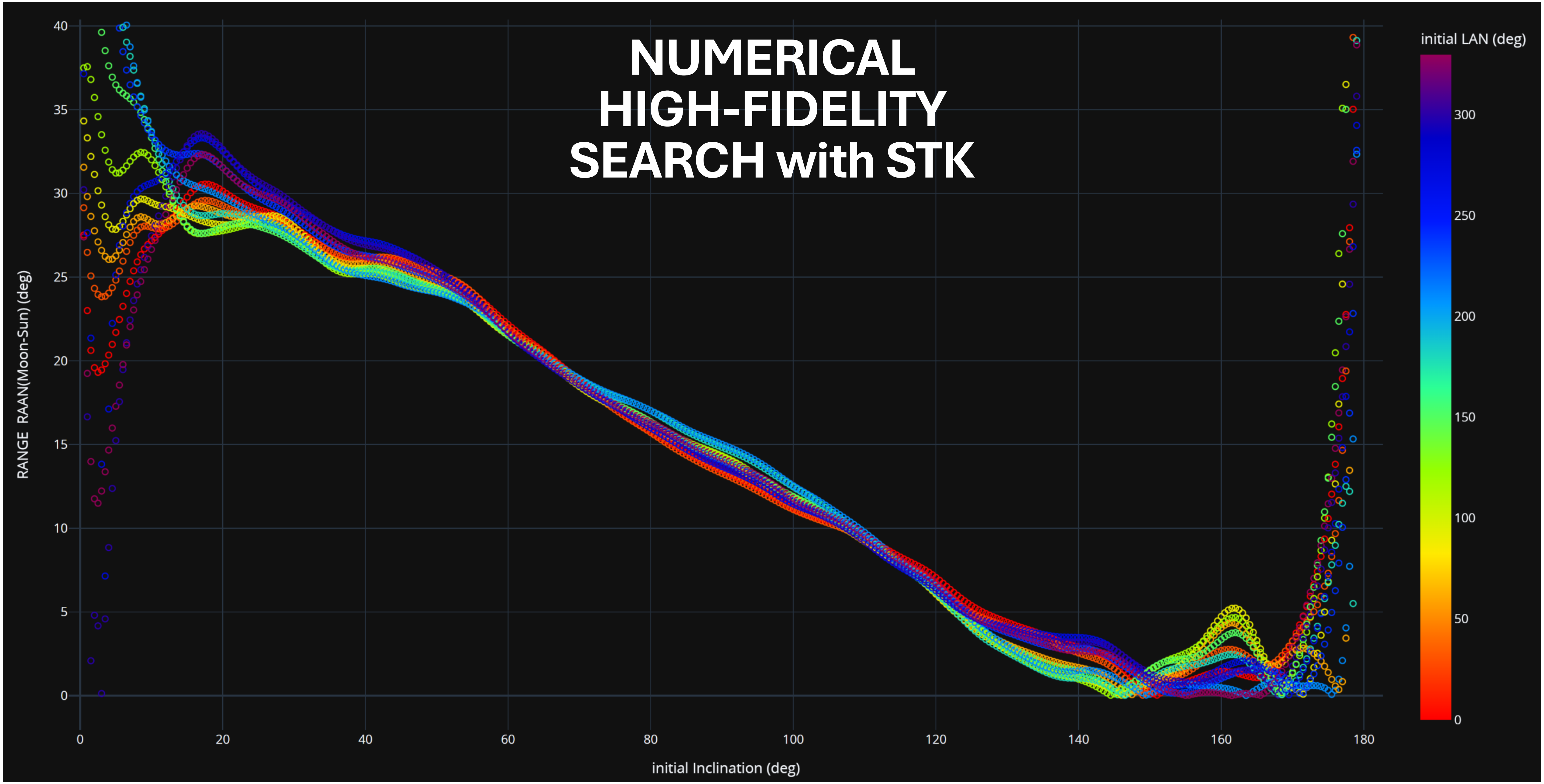

Figure 5. Full inclination scan of 100X210km low lunar orbit with 360-deg range in LAN considered to determine range of $RAAN_{Moon-Sun}$ and candidate lunar sunrise orbits.

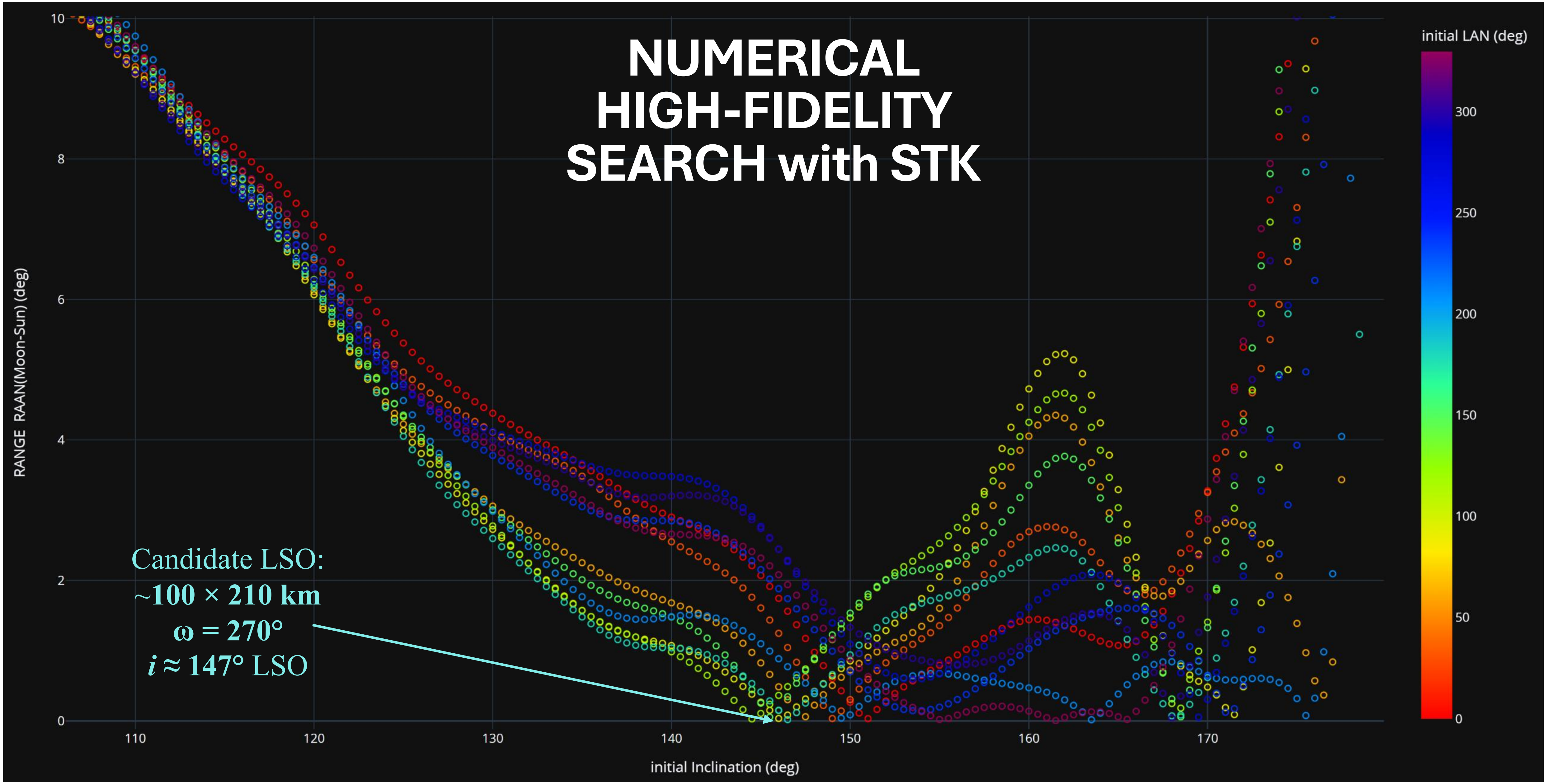

Figure 6. Full inclination scan of 100X210km low lunar orbit with 360-deg range in LAN considered to determine range of $RAAN_{Moon\text{-}Sun}$. Zoomed in near minimum values of $RAAN_{Moon\text{-}Sun}$ range to identify candidate lunar sunrise orbits.

LOW LUNAR ORBIT
CORRECTION MANEUVERS
FOR SUNRISE RETARGETING

Sun-Synchronous Drift Through J_6 & C_{22}

This section reaches the same candidate from the opposite direction: instead of measuring the node's swept range in a full-ephemeris propagation, it solves for the inclination whose secular nodal rate equals the solar rate in a spherical-harmonic field, recovering $i \approx 147$ deg (Figure 7).

The sunrise condition holds the orbit plane fixed relative to the Sun, so the node must precess at the selenocentric solar rate:

$$\Omega_{\odot} = 2\pi / T_{\oplus} \approx 0.9856\ °/\text{day}$$

$T_{\oplus}$ - synodic period (apparent solar motion)

Supplied by the even zonal harmonics (J_2, J_4, J_6), retained through degree six:

$$\Omega = \Omega_{J_2} + \Omega_{J_4} + \Omega_{J_6}$$

$$\Omega_{J_2} = -(3/2)\ n\ J_2\ (R/p)^2 \cdot \cos i$$

$$\Omega_{J_4} = (15/16)\ n\ J_4\ (R/p)^4 \cdot \cos i\ (4 - 7 \sin^2 i)$$

$$\Omega_{J_6} = -(105/128)\ n\ J_6\ (R/p)^6 \cdot \cos i\ (33 \sin^4 i - 36 \sin^2 i + 8)$$

i - inclination
n - mean motion
R - lunar reference radius (≈ 1737.4 km)
p - semi-latus rectum, $p = a(1 - e^2)$

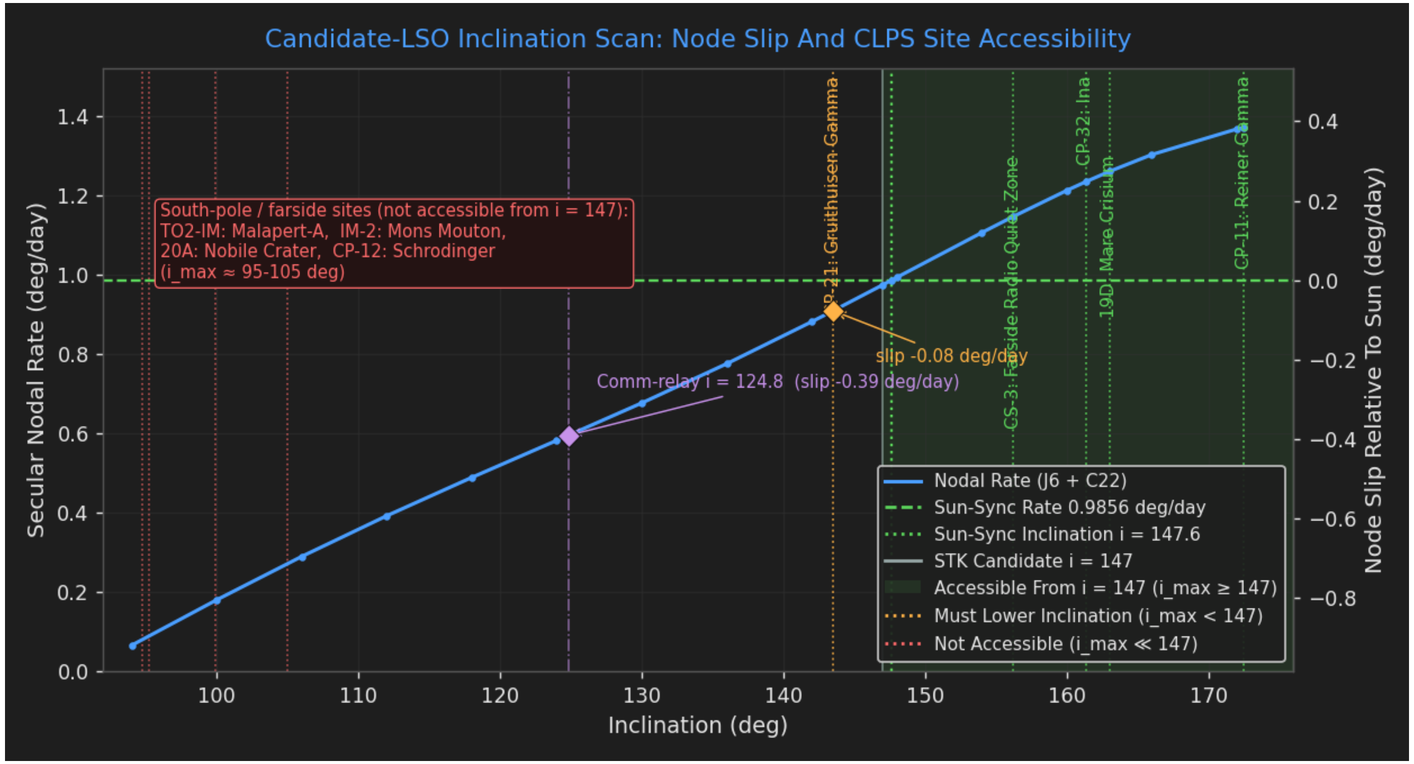

Figure 7. Secular nodal rate vs. inclination (degree-6 + C_{22}); node slip from the Sun on the right axis.

- Balance crosses the sun-synchronous rate at $i \approx 147.6°$ — consistent with the 147° staging value; shaded $i \geq 147°$ is reachable.
- Site node slip: Reiner Gamma / Mare Crisium / Ina / CS-3 ≈ 0; Gruithuisen 143.5° (−0.08°/day); comm-relay 124.8° (−0.39°/day).

J_2 alone → 155°; $+J_4+J_6$ → ***i* ≈ 147.6°.** C_{22} gives no inertial secular nodal drift, but synchronous rotation fixes the Earth-pointing bulge in the body frame → residual drift depends on synodic phase; apsidal drift fixes perilune latitude. Both are removed by a numerical trim.

Sunrise-Retargeting Maneuver Sequence

Because the sunrise epoch is fixed by the Sun and independent of the orbit, lighting maps one-to-one to when the spacecraft is overhead. The recovery reduces to placing the overflight inside the fixed post-sunrise window with an in-track phasing maneuver — arrival time is adjusted without rotating the plane.

$$\tau_{as} = t_{sr} - t_{fly}, \quad \tau_{as} \in (0, 24\text{ h}]$$

$$\partial\tau_{as} / \partial t_{fly} = \mathbf{1}$$

τ_{as} - interval after sunrise

τ_{sr} - sunrise epoch at site

τ_{fly} - overflight epoch

1 · Establish

Tangential burn at the node nearest the approach corridor sets up the phasing orbit.

→

2 · Coast N revs

Coast N revolutions; the node and apse drift at the secular rates above.

→

3 · Restore + trim

Equal-and-opposite burn restores the staging orbit; a small trim removes the coast drift.

$$\Delta V_{\varphi} = n\,\Delta a = (2V/3)\cdot|\Delta\tau_{as}| / (N P), \quad D = N P, \quad \Delta T = (3T/2a)\,\Delta a \quad (V \approx 1.61\text{ km/s}, P \approx 2.05\text{ hr})$$

ΔV_{φ} – two burn sequence ΔV cost

D - two burn sequence elapsed time

NEAR-TERM

Several successive dawn overflights spaced by one orbital period — a missed descent is often recovered at a later pass for free, or with a few-orbit phasing correction.

CROSS-MONTH

Off-nominal delivery misses the first sunrise; the next recurs one lunar day (≈ 29.5 d) later. A single phasing burn walks the track back — control authority ≈ 24 km per m/s over ~345 rev.

Cross-Month Ground-Track Correction

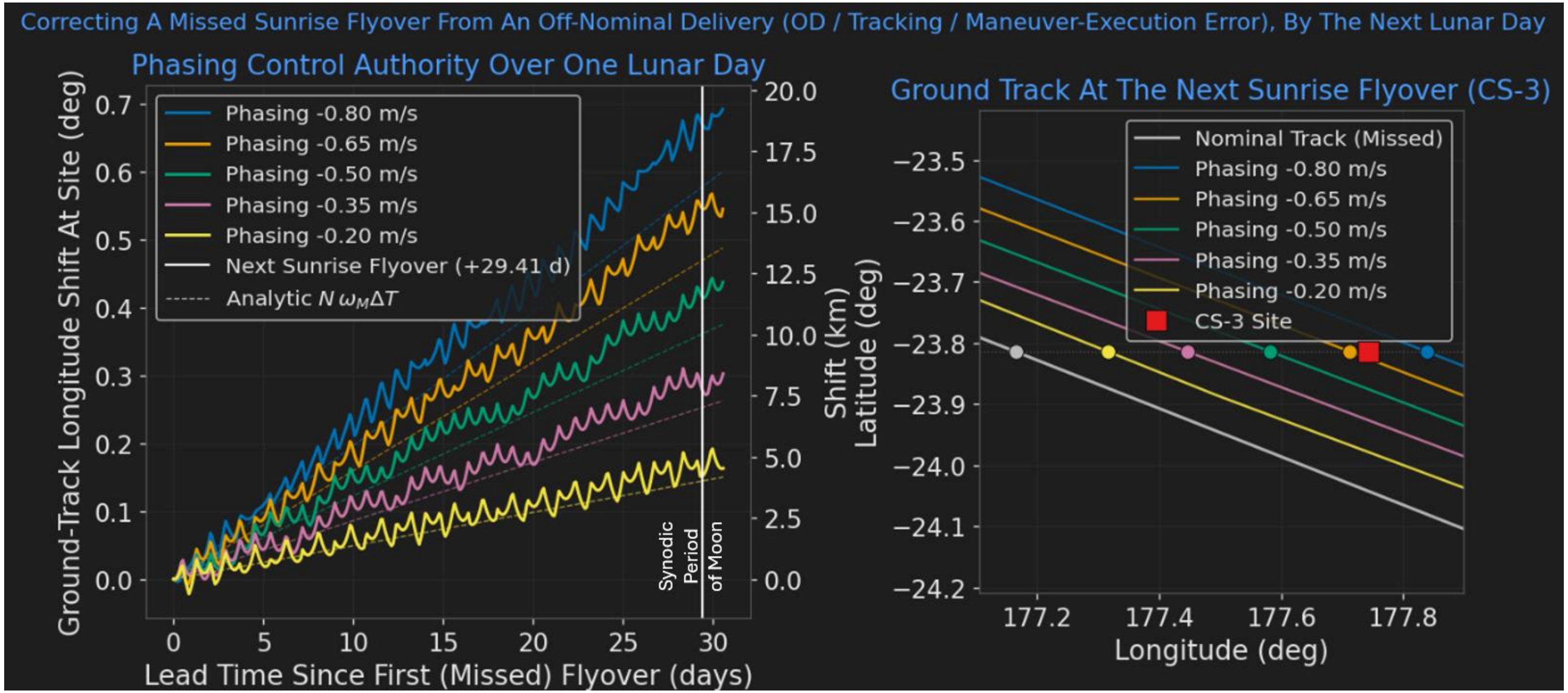

Figure 8. Correcting a missed sunrise flyover by in-track phasing (candidate i = 147.6 deg): overflight longitude shift (left) and ground tracks near CS-3 (right).

≈ 15 km
residual miss (sun-sync geometry repeats)

−0.65 m/s
centers the descending pass on CS-3

- A single tangential phasing burn biases the orbital period; the along-track offset accumulates over revolutions, shifting the sub-satellite crossing in longitude ∝ burn magnitude × revs.
- One lunar day (~345 rev): **control authority ≈ 24 km per m/s of phasing ΔV**, numerical agrees with analytic estimate within the per-rev libration (left panel).
- Sun-synchronous candidate (i = 147.6°): the plane tracks the Sun, so geometry repeats lunar-day to lunar-day and the residual miss stays small (~15 km).
- Biases of −0.2 to −0.8 m/s walk the next-sunrise track eastward in steps < 20 km; ≈ −0.65 m/s centers the descending pass on CS-3 (right panel).
- The correction is purely along-track; a node cross-track error would need a small plane change (out of scope here).

Recovery Cost vs. Available Lead Time

- Propagator-targeted: each point is root-found so a propagated site-latitude crossing lands on the site in the full degree-6 + C_{22} field with Earth third-body — not a linear estimate.

- Three orbits:
    - Sun-sync candidate (i = 147°, 100×210 km)
    - Off-sun-sync farside (i = 124.8°, 108 km)
    - Gruithuisen-serving (i = 142.5°, 100×210 km)

- Feasibility limit $|\Delta a| \leq 60$ km (small-phasing). Feasible recoveries occur only at natural ground-track recurrences.
- At shorter lead times no phasing solution exists (crosses): closing the miss that fast would need $|\Delta a| > 1000$ km — a plane change or large altitude change.
- Gruithuisen is the most constrained: its site sits at the orbit's turning latitude, so it recovers only at one lunar day — motivating a small inclination margin (147 → 143.5°).

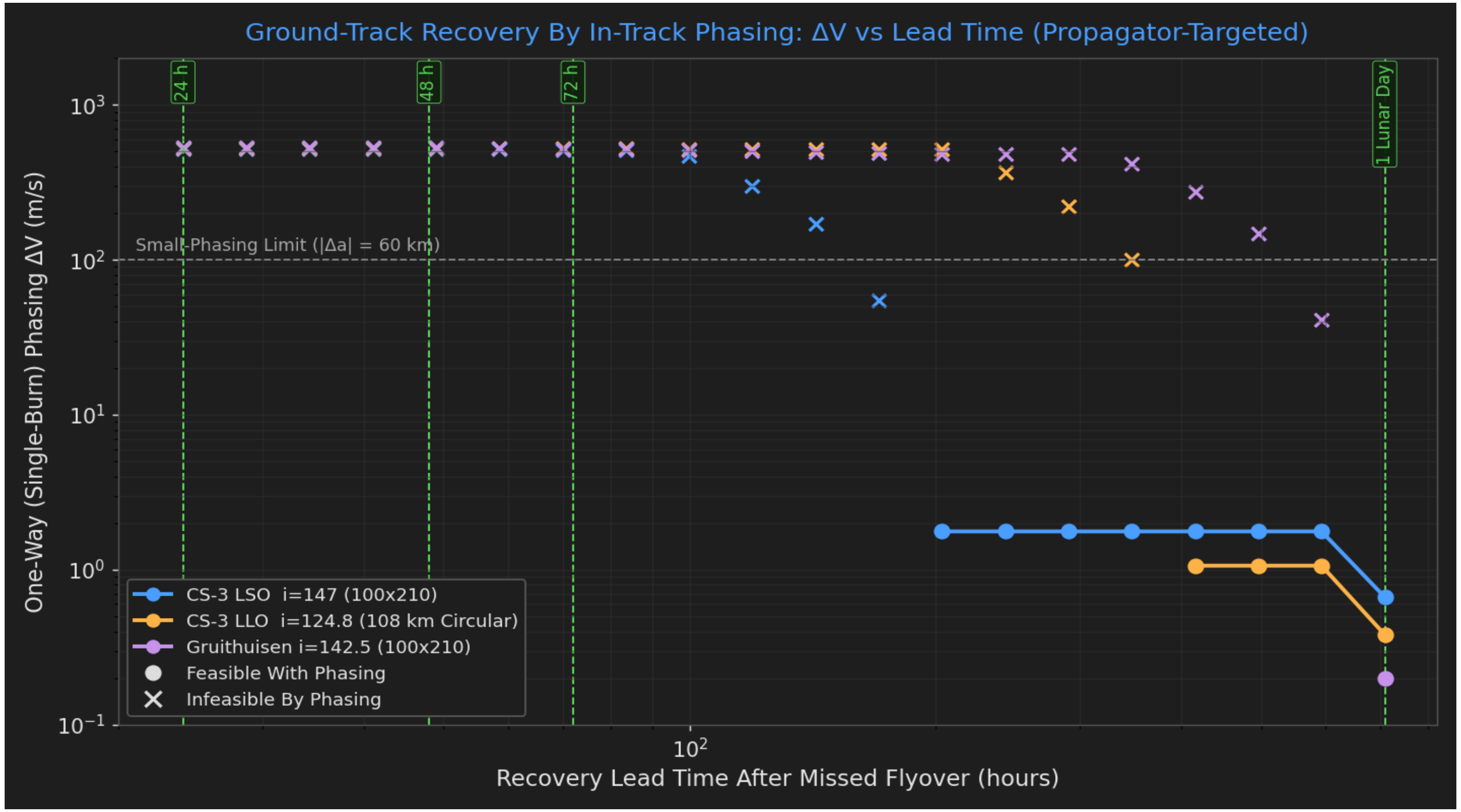

Figure 9. Single-burn phasing ΔV vs. lead time for three orbits (propagator-targeted).

< 2 m/s at a natural recurrence, falling to **0.2–0.67 m/s** by one lunar day.

Applying the Candidate LSO to CLPS Missions

* The sun-synchronous inclination also fixes the reachable latitude band: a retrograde LSO reaches a maximum latitude of 180° − i, so the i = 147° candidate serves sites within ~33° of the equator.

* Mid-latitude sites are reached by the candidate at ≈ 0 node slip; a missed sunrise descent is recovered at the next lunar dawn by a small in-track phasing burn (a few tenths m/s). The binding constraint is ground-track placement, not sunrise timing.

REACHABLE LATITUDE BAND

$$lat_{max} = 180° - i \rightarrow \pm 33° \ (i = 147°)$$

South-pole and farside-polar sites (Malapert-A, Mons Mouton, Nobile, Schrödinger) fall outside this band and are not served by the candidate.

REPRESENTATIVE CLPS LANDING SITES SERVED BY THE CANDIDATE LSO

Mission	Landing site	Lat, Lon (deg)	Status	Served by
Blue Ghost M1	Mare Crisium	+17.0, +59.1	Landed 2025	i = 147° · ≈ 0 slip
IM-3 (CP-11)	Reiner Gamma	+7.5, −59.0	Planned	i = 147° · ≈ 0 slip
CP-32	Ina	+18.7, +5.3	Planned	i = 147° · ≈ 0 slip
Blue Ghost M2 (CS-3)	Farside radio-quiet zone	−23.8, −177.7	Planned 2027	i = 147° · ≈ 0 slip
Blue Ghost M3 (CP-21)	**Gruithuisen Γ**	**+36.5, −40.8**	**Planned 2028**	**i = 143.5° · −0.08°/day**

Comm-relay coverage may instead hold i ≈ 124.8° (−0.39°/day) — furthest from sun-synchronicity and the largest station-keeping budget of the cases considered.

CLPS CS-3 Farside Mission: Two Relay Architectures

CS-3 (Blue Ghost M2) deploys a communications-relay satellite into an elliptical frozen orbit before descending to the farside radio-quiet zone (−23.8°, −177.7°). Two staging architectures were examined.

Architecture A · Sun-Synchronous LSO (i = 147°)

84-day lifetime, no station-keeping · **up to 3** dawn attempts

- Relay dropped in an elliptical orbit at 750 km perilune, at the same 147° inclination, so the LLO is a true LSO.
- Fixed repeat ground track over the site (Fig. 11); geometry viewed in the Moon–Sun rotating frame (Fig. 10).

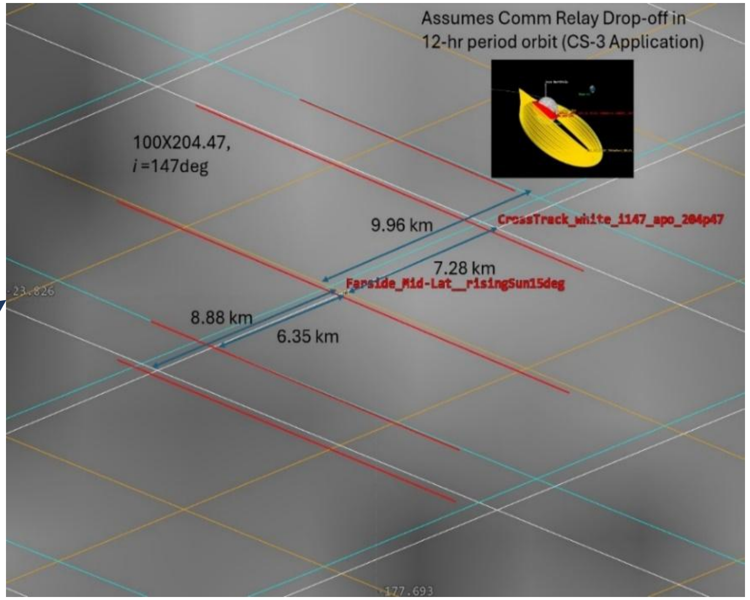

Figure 11. Nearly dawn-repeating ground track (i = 147°).

Architecture B · Frozen Inclination, LAN-Rotating ($i \approx$ 124.8°)

100 → 108 km altitude tune preserves the relay's frozen inclination

- Matches the comm-relay frozen inclination for coverage; sunrise flyovers come from a 360° LAN rotation each lunar dawn (Fig. 12) — not a true fixed RGT.
- Iterating LLO altitude yields near-repeating tracks, adding backup dawn windows while minimally changing the nominal mission.

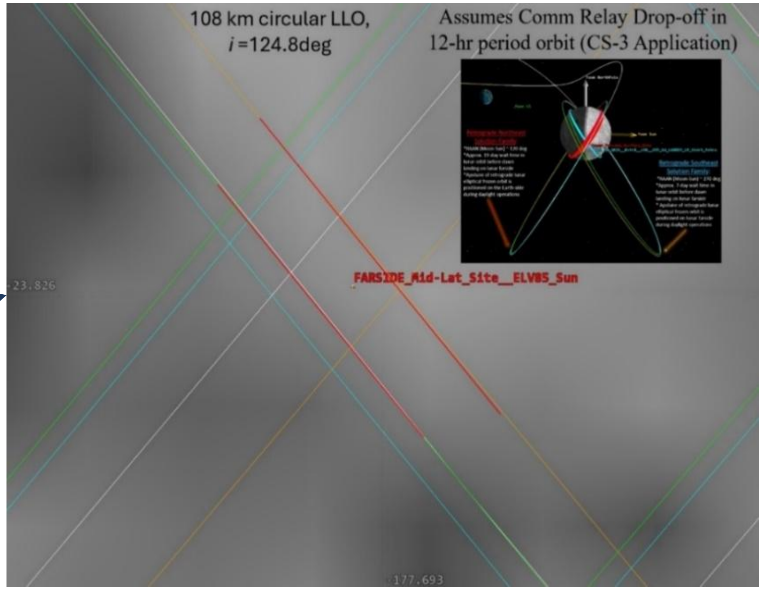

Figure 12. Dawn-repeating ground track via LAN rotation (i = 124.8°).

CLPS CS-3 Farside Mission Relay Architecture:

Staging Architecture A · Sun-Synchronous LSO ($i = 147°$)

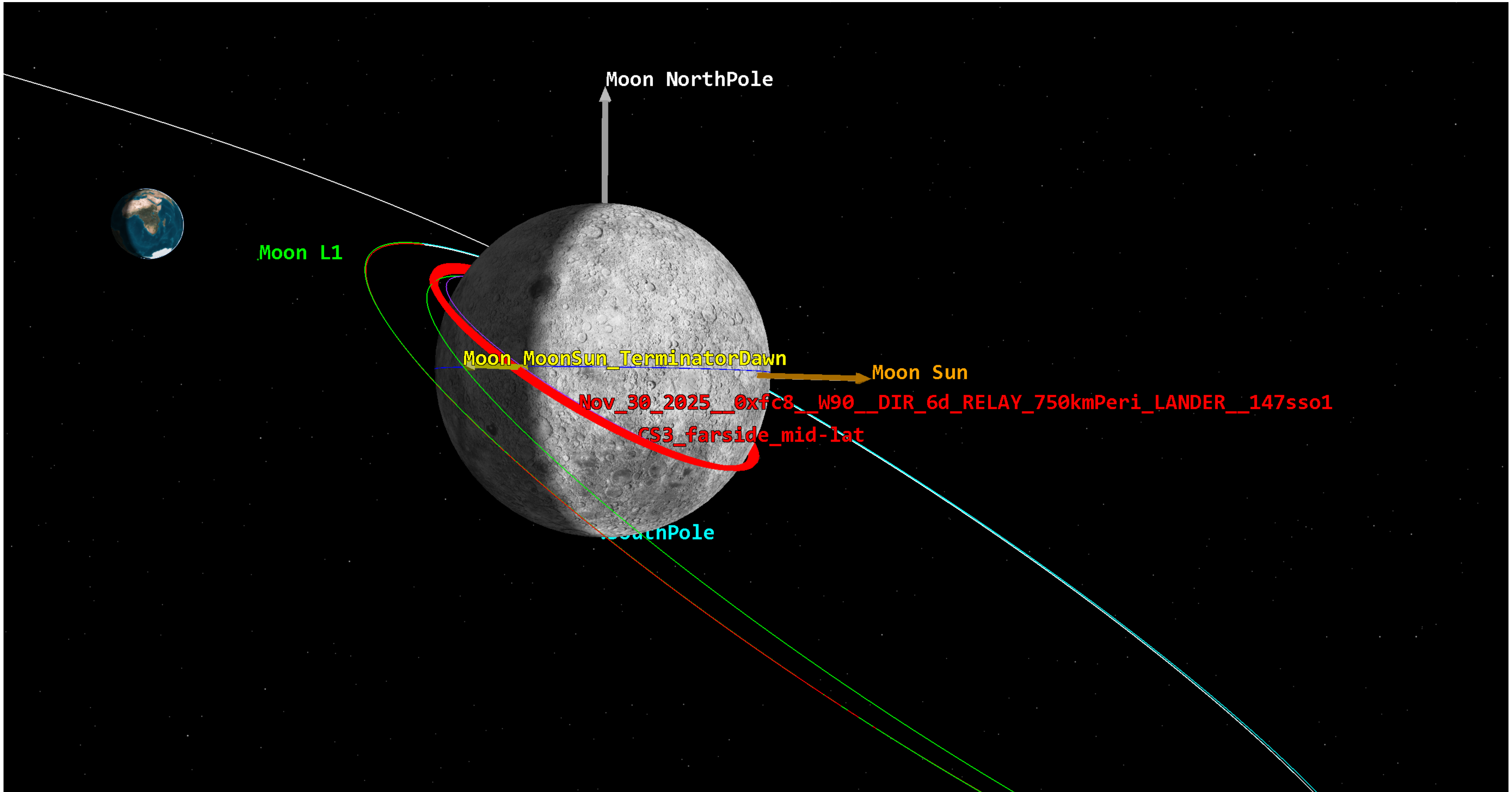

Figure 10. CS-3 application: communications relay satellite dropped off elliptical lunar orbit with 750 km perilune altitude, while LSO inclination = 147 degrees with orbit lifetime of 84 days. Viewed in Moon-Sun rotating frame.

Key Takeaways

- A sun-synchronous, repeat-ground-track LSO turns a missed lunar-dawn descent into a near-zero-cost contingency: recovery nudges an overflight already near the dawn window rather than forcing a dawn return from an arbitrary orbit.
- The sun-synchronous inclination is set by even zonal harmonics through J6 → $i \approx 147.6°$ (J2-only gives 155°); C_{22} and apsidal drift add a synodic-phase-dependent residual removed by a numerical trim.
- Lighting maps one-to-one to overflight timing ($\partial \tau as/\partial tfly = 1$), so recovery is a pure in-track phasing maneuver — no plane rotation.
- Near-term: several successive dawn passes, often free or a few-orbit correction. Cross-month: one phasing burn over ≈ 29.5 days; control authority ≈ 24 km per m/s, residual miss ~15 km → biases of a few tenths m/s (−0.65 m/s recenters CS-3).
- Feasible only at natural recurrences ($|\Delta a| \leq 60$ km, < 2 m/s); it cannot be rushed by phasing. Carry a small inclination margin for sites near the turning latitude (Gruithuisen).
- Directly applicable to mid-Latitude CLPS sites (Mare Crisium, Renier Gamma, Ina, CS-3) at ≈0 node slip; Gruithuisen needs $i = 143.5°$, and CS-3's comm relay case can instead hold $i \approx 124.8°$ with LAN rotation.

0.2–0.67 m/s

recover at one lunar day

≈ 24 km / (m/s)

cross-month control authority

$i \approx 147.6°$

sun-synchronous inclination

$|\Delta a| \leq 60$ km

phasing-feasible regime

Conclusions

* **Lunar Sunrise Orbits (LSOs)** provide a new mission architecture that preserves both **repeat ground tracks and local sunrise lighting**, enabling resilient CLPS landing operations.

* Medium-fidelity RTBP+NS orbit families exhibit the same repeatability and stability trends observed in independent high-fidelity STK simulations, increasing confidence that these orbit families are physically realizable.

    * Candidate **100 × 210 km, ω = 270°, *i* ≈ 147°** LSO identified and validated using STK high-fidelity & nodal-rate analyses

* Missed descent opportunities can be recovered using **simple in-track phasing maneuvers** without rotating the orbital plane or nominal mission architecture.

* One lunar-day recovery provides approximately **24 km of ground-track correction per 1 m/s** of phasing ΔV; representative recoveries require only **~0.2–0.67 m/s**.

* LSO concepts increase **CLPS mission robustness** by providing low-cost backup sunrise landing opportunities while preserving thermal and power constraints to support **multiple mid-latitude CLPS landing sites**, including Mare Crisium, Reiner Gamma, and the farside radio-quiet zone.

Appendix

REPRESENTATIVE LUNAR SUNRISE ORBIT RESULTS

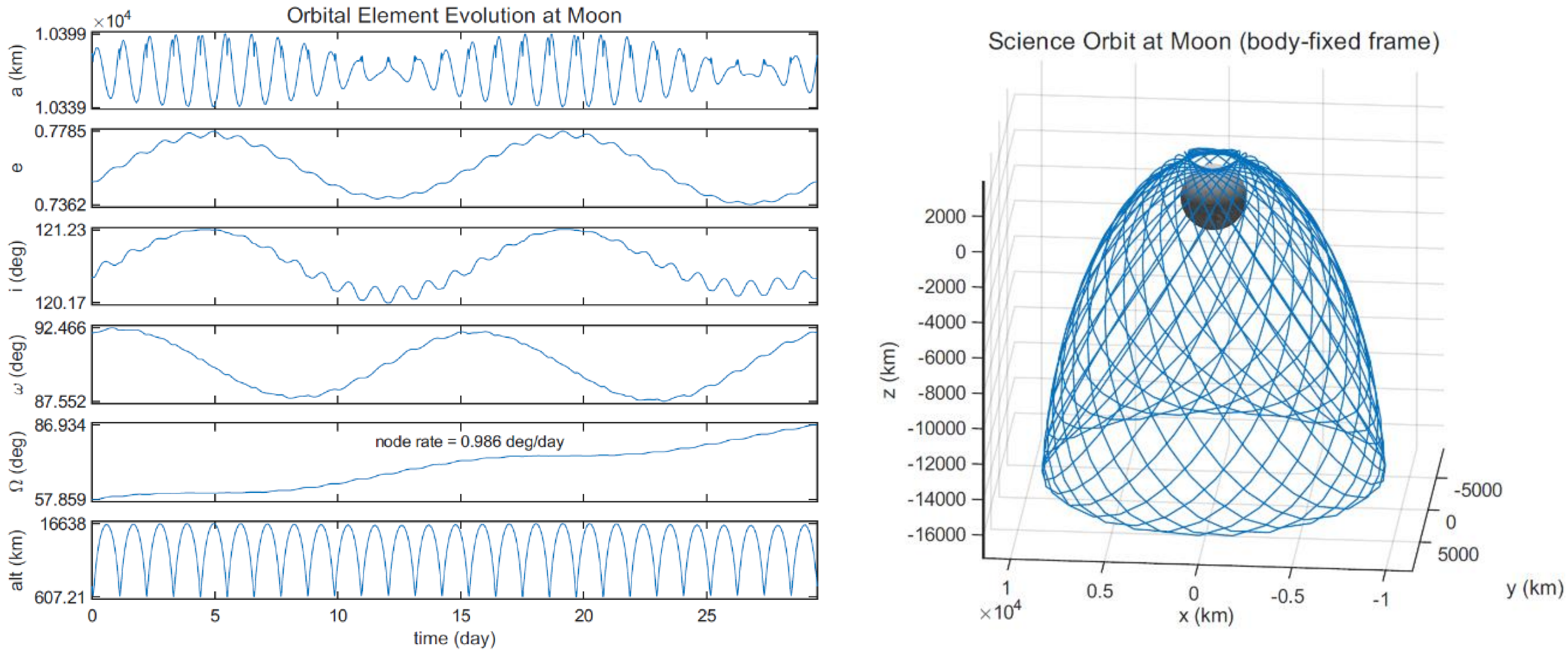

Figure 3: Representative $N = 27$ classic frozen LSO.

b1 = 1.0459519179817418 & b2 = 2.0000052854972177

REPRESENTATIVE LUNAR SUNRISE ORBIT RESULTS

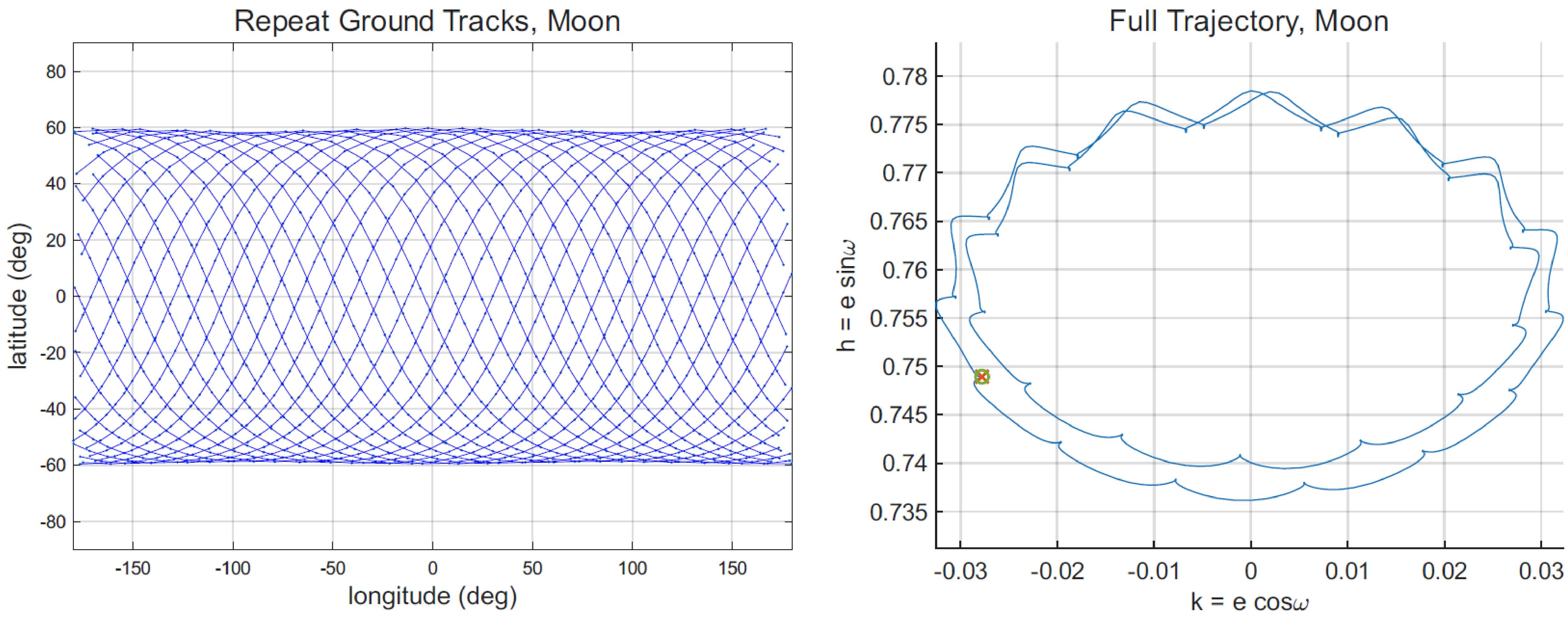

Figure 3: Representative $N = 27$ classic frozen LSO.

b1 = 1.0459519179817418 & b2 = 2.0000052854972177

REFERENCES

[1] Bussey, B. et al. (2019) *AGU Fall Meeting*. PA54B-11.

[2] National Aeronautics and Space Administration, "Commercial Lunar Payload Services," https://www.nasa.gov/commercial-lunar-payload-services/, 2025, Accessed: 2026-02-15.

[3] Russell, R. P. and Lara, M., "Long-Lifetime Lunar Repeat Ground Track Orbits," Journal of Guidance, Control, and Dynamics, Vol. 30, No. 4, 2007, pp. 982–993.

[4] Van Hammond, C. J., Russell, R. P., and Genova, A. L., "Sun-Synchronous Orbits at the Moon," AAS/AIAA Astrodynamics Specialist Conference, Boston, MA, 2026, AAS Paper 26-XXX.

[5] Konopliv, A. S., Park, R. S., Yuan, D. N., et al., "The JPL lunar gravity field to spherical harmonic degree 660 from the GRAIL Primary Mission," Journal of Geophysical Research: Planets, Vol. 118, No. 8, 2013, pp. 1415–1434, High-resolution lunar gravity field from GRAIL data.

[6] Pines, S., "Uniform Representation of the Gravitational Potential and its Derivatives," *AIAA Journal*, Vol. 11, No. 11, 1973, pp. 1508–1511.

[7] Szebehely, V., "Description of the Restricted Problem," Theory of Orbits: The Restricted Problem of Three Bodies, chap. 1, Academic Press, New York, 1967, See especially Sec. 1.4, "Equations of Motion in a Synodic Coordinate System and the Jacobian Integral".

[8] McArdle, S. and Russell, R. P., "Stable Low Altitude Lunar Periodic Orbits Using the GRAIL Gravity Field," AAS/AIAA Astrodynamics Specialist Conference, 2019.

[9] Lara, M., "On the frozen orbits of a satellite," Celestial Mechanics and Dynamical Astronomy, Vol. 101, 2008, pp. 389–399.

[10] McArdle, S. and Russell, R. P., "Circulating, Eccentric Periodic Orbits at the Moon," Celestial Mechanics and Dynamical Astronomy, 2021.

[11] Genova, A. L., Morrison-Fogel, D., & Levinson-Muth, P., "Transfers from TLI to Lunar Frozen Orbits with Applications to NASA's CLPS & Artemis Programs," AAS/AIAA Space Flight Mech. Mtg., Orlando, FL, Jan. 8-12, 2024.

[12] Zuber, M. T., Smith, D. E., Watkins, M. M., & Binder, A. B., "Gravity Field of the Moon from the Gravity Recovery and Interior Laboratory (GRAIL) Mission," Science, 2013.

[13] Genova, A. L., Morrison-Fogel, D., Levinson-Muth, P., Dono Perez, A., & Blue, R., "Lunar Browser trajectory tool," Software for the NASA Science Mission Directorate Workshop," Washington, DC, May 7-9, 2024.

[14] Vallado, D. A., Fundamentals of Astrodynamics and Applications, 4th ed., Microcosm Press, Hawthorne, CA, 2013, Chap. 6.

REFERENCES

Genova, A. L., “Linking Lunar Orbital Dynamics to Planetary Protection Policy,” *Invited Talk* at National Academy of Sciences: Committee on Planetary Protection Panel, *Space Science Week*, March 25, 2026.

Morrison-Fogel, D., Genova, A. L., Levinson-Muth, P., & Blue, R., “Lunar Browser Utilization of Machine Learning for Trajectory Solution Production,” AAS/AIAA Space Flight Mechanics Meeting, Kaua’i, HI, Jan. 19-23, 2025.

Robinson, M. S., Dunham, D. W., Cheung, K., Genova, A. L., et. al, “Swirl mission concept: Unraveling the enigma,” *Planetary and Space Science*, Vol. 162, pp. 73-88, Nov. 1, 2018.

Genova, A. L. et. al, “Trajectory Design from GTO to Lunar Equatorial Orbit for the Dark Ages Radio Explorer Spacecraft,” AAS/AIAA Space Flight Mechanics Meeting, Williamsburg, VA, Jan. 11-15, 2015.

Genova, A. L., Kaplinger, B., Wilde, M., & Aldrin, B., “Establishment and Design of an Earth-Moon Communications Network in Lunar Polar Orbit,” IEEE Aerospace Conference, Big Sky, MT, Mar. 3-10, 2018.

Hardgrove, C., “The Lunar Polar Hydrogen Mapper (LunaH-Map) CubeSat Mission”, no. 1903, p. 2654, 2016.
The lunar polar hydrogen mapper (lunah-map) cubesat mission

Genova, A. L., & Dunham, D. W., “Trajectory Design for the LunaH-Map CubeSat,” Proceedings of the 27th Presented at 27th AAS/AIAA Space Flight Mechanics Meeting, San Antonio, TX, Feb. 5-9, 2017.

Genova, A. L, “Existence of Ballistic Capture Transfer Trajectories from Trans-Lunar Injection to Lunar Polar Orbit for all Lunar Phases at Time of Departure,” Ph.D. dissertation, Florida Institute of Technology, December 2020.

Genova, A. L. et. al, “Lunar Orbit Evolution and Strategies for Planetary Protection,” COSPAR Scientific Assembly, Florence, Italy Aug. 1-9, 2026